JOURNAL OF TISSUE ENGINEERING AND REGENERATIVE MEDICINE
J Tissue Eng Regen Med 2009; **3**: 37–42.
Published online 19 November 2008 in Wiley InterScience (www.interscience.wiley.com) **DOI:** 10.1002/term.132

RESEARCH ARTICLE

Hierarchical starch-based fibrous scaffold for bone tissue engineering applications

Albino Martins[1,2]*, Sangwon Chung[1,2], Adriano J. Pedro[1,2], Rui A. Sousa[1,2,3], Alexandra P. Marques[1,2], Rui L. Reis[1,2,3] and Nuno M. Neves[1,2]

[1]*3B's Research Group – Biomaterials, Biodegradables and Biomimetics, Department of Polymer Engineering, University of Minho, and Headquarters of the European Institute of Excellence on Tissue Engineering and Regenerative Medicine, AvePark, Zona Industrial da Gandra, S. Cláudio do Barco, 4806-909 Caldas das Taipas, Guimarães, Portugal*
[2]*Institute for Biotechnology and Bioengineering (IBB), PT Government Associated Laboratory; Braga, Portugal*
[3]*Stemmatters, Biotechnology and Regenerative Medicine Ltd, AvePark, Zona Industrial da Gandra, S. Cláudio do Barco, Apartado 4152-4805 Caldas das Taipas, Portugal*

Abstract

Fibrous structures mimicking the morphology of the natural extracellular matrix are considered promising scaffolds for tissue engineering. This work aims to develop a novel hierarchical starch-based scaffold. Such scaffolds were obtained by a combination of starch–polycaprolactone micro- and polycaprolactone nano-motifs, respectively produced by rapid prototyping (RP) and electrospinning techniques. Scanning electron microscopy (SEM) and micro-computed tomography analysis showed the successful fabrication of a multilayer scaffold composed of parallel aligned microfibres in a grid-like arrangement, intercalated by a mesh-like structure with randomly distributed nanofibres (NFM). Human osteoblast-like cells were dynamically seeded on the scaffolds, using spinner flasks, and cultured for 7 days under static conditions. SEM analysis showed predominant cell attachment and spreading on the nanofibre meshes, which enhanced cell retention at the bulk of the composed/hierarchical scaffolds. A significant increment in cell proliferation and osteoblastic activity, assessed by alkaline phosphatase quantification, was observed on the hierarchical fibrous scaffolds. These results support our hypothesis that the integration of nanoscale fibres into 3D rapid prototype scaffolds substantially improves their biological performance in bone tissue-engineering strategies. **Copyright © 2008 John Wiley & Sons, Ltd.**

Received 2 September 2008; Accepted 14 September 2008

Keywords **electrospinning; rapid prototyping; starch-based fibres; micro/nano multilayer scaffolds; human osteoblastic cells; bioreactor**

1. Introduction

Biodegradable scaffolds are generally recognized as indispensable elements in tissue engineering and regenerative medicine strategies. Scaffolds are used as temporary templates for cell seeding, migration, proliferation and differentiation prior to the regeneration of biologically functional tissue or natural extracellular matrix (ECM) (Lutolf and Hubbell, 2005; Hutmacher *et al*., 2007). Ideally, to create a tissue-engineered construct capable of regenerating a fully functional tissue, it should mimic both the fibrous form and the complex function of the native ECM (Agrawal and Ray, 2001). Like natural ECM, a range of topographic features at the macro-, micro- and even nano-scale levels must lead cell response (Norman and Desai, 2006). A multi-scale network structure can be developed by integrating microfibrous structures, produced by wet-spinning or rapid prototyping, with electrospun nanofibres (Tuzlakoglu *et al*., 2005; Santos *et al*., 2007; Moroni *et al*., 2008).

Electrospun fibres typically have dimensions varying from the nano- to the micro-scale, although fibre diameters in the sub-micrometer range are mainly

*Correspondence to: Albino Martins, 3Bs Research Group – Biomaterials, Biodegradables and Biomimetics, Department of Polymer Engineering, University of Minho, Portugal.
E-mail: amartins@dep.uminho.pt

observed (Huang *et al*., 2003). These mesh-like scaffold are characterized by high porosity, high surface : volume ratio and, most importantly, they can closely mimic the morphology of the native ECM of many tissues. Such physical cues enhance cell adhesion, proliferation and differentiation, and consequently neo-tissue formation on nanofibrous meshes of both natural and synthetic polymers (Zhang *et al*., 2005; Martins *et al*., 2007).

Rapid prototyping has emerged as a powerful polymer-processing technique for the production of scaffolds in the area of tissue engineering (Hutmacher *et al*., 2004; Leong *et al*., 2003; Mironov *et al*., 2003; Peltola *et al*., 2008; Pfister *et al*., 2004; Yang *et al*., 2002; Yeong *et al*., 2004). The main advantage of this technique is the possibility of creating structures with customized shapes linked with computer-aided design (CAD), thus providing more flexibility, versatility and reproducibility in creating scaffolds (Hutmacher *et al*., 2004; Moroni *et al*., 2005; Moroni *et al*., 2006; Capes *et al*., 2005). However, the typical pore size of RP scaffold constitutes a limitation in the cell-seeding efficiency (Pfister *et al*., 2004), once it is relatively large as compared to cell dimensions.

Therefore, the aim of this study was to characterize a novel hierarchical starch-based fibrous scaffold obtained by the combination of starch–polycaprolactone (SPCL) micro- and polycaprolactone (PCL) nano-motifs, respectively produced by rapid prototyping (RP) and electrospinning. The defined strategy aimed at overcoming the high number of cells needed to attain sufficient adherent cells to the RP scaffolds (Moroni *et al*., 2008), which can be accomplished by alternately integrating electrospun nanofibre meshes every two consecutive layers of plotted microfibres. In this way these nanofibre meshes will act as cell entrapment systems, increasing cell attachment efficiency, cell proliferation and tissue regeneration. Ultimately, this integration will enhance the potential application of such three-dimensional (3D) fibrous structures in bone tissue-engineering strategies. This work reports the results of a set of experiments in which human osteoblast-like cells were dynamically seeded and statically cultured for 7 days on micro-nano fibre polymeric scaffolds designed to validate this hypothesis.

2. Materials and methods

2.1. Scaffold fabrication

Three-dimensional (3D) rapid prototyping scaffolds (6RP) were fabricated using a 3D plotting technique (Bio-plotter, EnvisionTec GmbH, Germany), using a 30 : 70 (wt%) blend of starch and polycaprolactone (SPCL, Novamont, Italy). SPCL polymer powder was placed into a metal barrel and heated at 140 °C through a heated cartridge unit, then plotted through a nozzle by air pressure control. The nozzle comprises a stainless steel needle with internal diameter 0.5 mm and length 6 mm. A metal piston plunger with a Teflon seal was used to apply pressure to the molten polymer. The machine was linked to CAD software (PrimCam, Germany) which required inputs of dispensing and processing parameters (e.g. speed of the head, dispensing pressure and temperature) and the design parameters of the scaffold (e.g. scaffold dimensions, spacing between the polymer strands, and number of layers). The strand spacing was set to 1 mm, without offsets between the consecutive equivalent layers. The orientation was changed by plotting the polymer with 90° angle steps between two successive layers. The production of hierarchical fibrous scaffolds (6RP + 5NFM) was achieved by integrating nanofibre meshes (NFM) every two consecutive layers of plotted microfibres. The nanofibre meshes were previously produced by electrospinning, as described elsewhere (Araujo *et al*., 2007). Briefly, a polymeric solution of 17% w/v PCL, dissolved in an organic solvent mixture of chloroform : dimethylformamide (7 : 3 ratio), was electrospun by establishing a electric tension of 9.5 kV, a needle tip-to-ground collector distance of 200 mm and a flow rate of 1 ml/h. The scaffolds (6RP and 6RP + 5NFM scaffolds) were all cut into 5 × 5 mm cubical samples from the originally deposited bulk 20 × 20 mm cube (12 layers) and sterilized using ethylene oxide (EtO) before the cell culture assays.

2.2. Scaffold characterization

Scaffold architecture was analysed using micro-computed tomography (μ-CT) with a desktop micro CT scanner (SkyScan 1072, Aartselaar, Belgium). The scanner was set to a voltage of 40 kV and a current of 248 μA, and the samples were scanned at 8.71 μm pixel resolutions by approximately 350 slices covering the sample height of 2.5 mm. For imaging, the sliced 2D tomographic raw images were reconstructed using CT Analyser software, and the threshold levels of the greyscale images were equally adjusted for all the samples to allow the measurement of the volume of pores, providing the data for scaffold porosity. 3D modelling was also used to analyse the scaffold structure in a non-destructive manner, using imaging software. The morphology of the scaffold was also analysed, using scanning electron microscopy (SEM; Leica Cambridge, Model S360, UK). All samples were previously sputter-coated with gold (Sputter Coater, Model SC502, Fisons Instruments, UK).

2.3. Cell seeding and culture

Human osteosarcoma-derived cells [Saos-2 cell line, European Collection of Cell Cultures (ECACC), UK], were maintained in Dulbecco's modified Eagle's medium (DMEM; Sigma-Aldrich; Germany) supplemented with 10% heat-inactivated fetal bovine serum (Biochrom AG, Berlin, Germany) and 1% antibiotic–antimycotic solution (Gibco, UK). Cells were cultured in a humidified incubator at 37 °C in a 5% CO_2 atmosphere and the medium was routinely replaced every 3–4 days.

DOI: 10.1002/term

Confluent osteoblastic-like cells were harvested and dynamically seeded onto the polymeric scaffolds as follows. The combined and the RP (controls) scaffolding structures were placed between stainless steel holding wires in spinner flasks (12 scaffolds/spinner flask) containing a suspension of osteoblast-like cells with a concentration of 0.5×10^6 cells/ml in a total volume of 35 ml. The stirrer was set at 80 r.p.m. and the spinner flasks left on for 72 h to allow the cells to colonize the entire scaffold. After this time period the osteoblasts/scaffold constructs were transferred to 24-well cell culture plates (Costar®, Corning, NY, USA) and statically cultured for 1 and 7 days under the culture conditions previously described for maintenance of the cell line.

2.4. Evaluation of cell adhesion, morphology and distribution

To evaluate the cell morphology, the cells–scaffold constructs were fixed with 2.5% glutaraldehyde (Sigma, USA) in phosphate-buffered saline (PBS; Sigma) solution for 1 h at 4 °C. Then, the samples were dehydrated through a graded series of ethanol and allowed to dry overnight. Finally, they were sputter-coated with gold (Model SC502, Fisons Instruments, UK) and observed in a scanning electron microscope (Model S360, Leica Cambridge, UK).

2.5. Cell viability assay

At each defined time culture period, the cell viability was determined using the CellTiter 96® Aqueous One Solution Cell Proliferation Assay (Promega, USA). This assay is based on the bioreduction of a tetrazolium compound, 3-(4,5-dimethylthiazol-2-yl)-5-(3-carboxymethoxyphenyl)-2-(4-sulphofenyl)-2*H*-tetrazolium (MTS), into a water-soluble brown formazan product. This conversion is accomplished by NADPH or NADH production by the dehydrogenase enzymes in metabolically active cells. The absorbance, measured at 490 nm in a microplate reader (Bio-Tek, Synergie HT, USA), is related to the quantity of formazan product and directly proportional to the number of living cells in the constructs. Three samples per type of scaffold and per time point were characterized.

2.6. DNA Quantification

Cell proliferation was evaluated by quantifying the total amount of double-stranded DNA throughout the culture time. Quantification was performed using the Quant-iT™ PicoGreen dsDNA Assay Kit (Invitrogen, Molecular Probes, OR, USA), according to the manufacturer's instructions, and after the cells in the construct were lysed by osmotic and thermal shock. The intensity of the fluorescence, proportional to the amount of double-strand DNA, was measured at an excitation wavelength of 485/20 nm and at an emission wavelength of 528/20 nm, in a microplate reader (Bio-Tek, Synergie HT, USA). Triplicates of each sample, allowed for a statistical analysis. The DNA concentration for each sample was calculated using a standard curve relating quantity of DNA and fluorescence intensity.

2.7. Alkaline phosphatase (ALP) quantification

To assess the osteogenic activity of cells seeded into the 3D scaffolds (6RP and 6RP + 5NFM), the expression of ALP was determined for both culture time periods, in the same samples used for DNA quantification. In each well of a 96-well plate (Costar®, Corning, NY, USA), 20 µl of each sample were mixed with 60 µl substrate solution and 0.2% wt/v *p*-nytrophenyl phosphate (Sigma, USA), in a substrate buffer of 1 M diethanolamine HCl (Merck, Germany) at pH 9.8. The plate was then incubated in the dark for 45 min at 37 °C. After the incubation period, 80 µl stop solution, 2 M NaOH (Panreac; Barcelona, Spain) plus 0.2 mM EDTA (Sigma), was added to each well. Standards were prepared with 10 µM/ml *p*-nytrophenol (pNP, Sigma, USA) solution, to obtain a standard curve covering the range 0–0.3 µM/ml. Triplicates of each sample and standard were made. Absorbance was read at 405 nm in a microplate reader (Bio-Tek, Synergie HT) and sample concentrations were read off from the standard curve. These ALP concentrations were normalized against the DNA concentrations of the same samples to determine the ALP activity.

2.8. Statistical analysis

Statistical analysis was performed using the SPSS statistic software (release 8.0.0 for Windows). First, a Shapiro–Wilk test was used to ascertain about data normality. Once biological results did not follow a normal distribution, Kruskal–Wallis test was performed to compare the effect of scaffold architecture over cell performance. In the analysis of the results, $p < 0.05$ was considered statistically significant.

3. Results and discussion

A novel hierarchical fibrous scaffold was developed, combining starch–polycaprolactone micro- and polycaprolactone nano-motifs, respectively produced by rapid prototyping (RP) and electrospinning (ES). These scaffolds were characterized by a 3D structure of parallel aligned rapid prototyped microfibres (average fibre diameter, 300 µm), periodically intercalated by randomly distributed electrospun nanofibres (fibre diameters in the range 400 nm–1.4 µm) (Figure 1B). When nanofibre meshes were integrated within the 3D scaffold, no

DOI: 10.1002/term

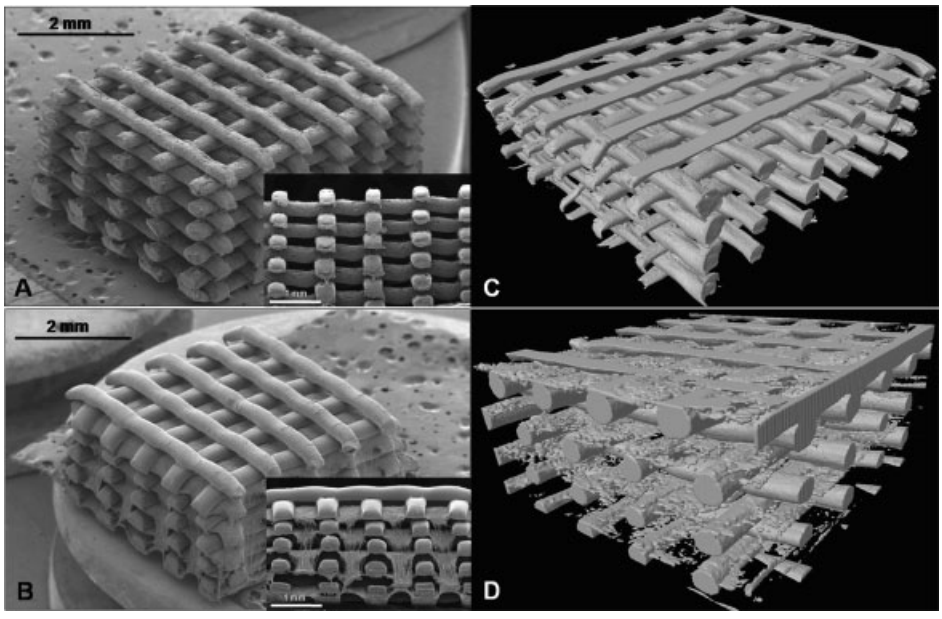

Figure 1. SEM and μ-CT micrographs of the starch-based rapid prototyped, 6RP (A, C) and hierarchical fibrous scaffolds, 6RP + 5NFM (B, D)

delamination between consecutive layers of RP fibres was observed, resulting in a stable scaffold. Additionally, this micro–nano scaffold architecture comprises a high-throughput scaffold process methodology, with regular control over RP-produced structure and nanofibres distribution within the scaffold. The integration of these nano-motifs resulted in a decrease of scaffold porosity of around 11% (from 79.4% on 6RP scaffolds to 68.3% on 6RP + 5NFM scaffolds), as determined by μ-CT analysis (Figure 1C, D). Despite a decrease in porosity, a fully interconnected porous structure was observed, allowing gas, nutrient and waste transport through the 3D structure.

Starch-based scaffolds have been proposed as candidates for bone tissue-engineering strategies in multiple studies (Gomes *et al.*, 2001, 2003, 2006, 2008; Salgado *et al.*, 2004, Salgado *et al.*, 2005, 2007; Tuzlakoglu *et al.*, 2005), supporting the choice of SPCL to develop the structures proposed in this study. Indeed, successful results were demonstrated in terms of cell viability, proliferation and maturation of osteoblastic cells or differentiation of bone marrow stromal cells. Moreover, other starch-based blends (corn starch, dextran and gelatine, 50 : 30:20 wt%) have already been used to produce different scaffold designs by 3D printing (3DP) (Lam *et al.*, 2002). Although showing suitable physicochemical properties for tissue-engineering applications, the biocompatibility of those 3DP geometric scaffolds, with a highly interconnected porous network, remains to be tested. The hierarchical starch-based fibrous scaffolds developed in the present study were seeded with human osteoblast-like cells to observe how the scaffold architecture affects their behaviour. Cells were initially allowed to attach to the scaffold using a dynamic system; this spinner flask bioreactor allows the cells to efficiently penetrate into the inner regions of the scaffolds, avoiding in a certain extent the preferential colonization of the outer most parts of the scaffolds (Oliveira *et al.*, 2007). Consequently, a homogeneous distribution of cells throughout the entire scaffold was observed. However, SEM micrographs demonstrated that osteoblastic cells preferentially adhered to the nanofibrous meshes (Figure 2B, D, G, H). This phenomenon of cellular preference was previously described by our group and others (Tuzlakoglu *et al.*, 2005, Kwon *et al.*, 2005, Yang *et al.*, 2005), when different cell types (osteoblastic, endothelial and neural stem cells) were seeded in micro- and nano-fibre-based scaffolds. Additionally, the integration of nanofibre meshes into the 3D rapid prototyped scaffolds seemed to act as a cell entrapment system within the RP scaffold. It was reported by others (Pfister *et al.*, 2004) that cells go through the pores of rapid prototyped scaffolds and accumulate at the bottom of the well plate during the seeding process, without attaching the scaffold, and thus reducing the seeding efficiency typically down to values of 25–35%. Thus, the integration of nanofibre meshes constitutes an innovative strategy to enhance cell seeding efficiency into 3D RP scaffolds.

The quantification of cell viability and metabolic activity of human osteoblast-like cells seeded into the combined electrospun nanofiber meshes and RP scaffolds was evaluated by MTS assay (Figure 3). The results revealed a steadily increasing trend, with culture time, although there was no significant difference on the effect of the type of scaffold architectures ($p > 0.05$). From the morphological evaluation of the constructs, it seems that the integrated nanofibre meshes into the 3D rapid prototyped structure also acted as a cell entrapment system within the scaffold. Consequently, a significant increment of cell proliferation and maturation, respectively assessed by DNA and ALP activity quantification, along the culture time, was observed on the hierarchical fibrous scaffolds (Figures 4, 5) in comparison to the rapid prototyped scaffolds ($p <$

DOI: 10.1002/term

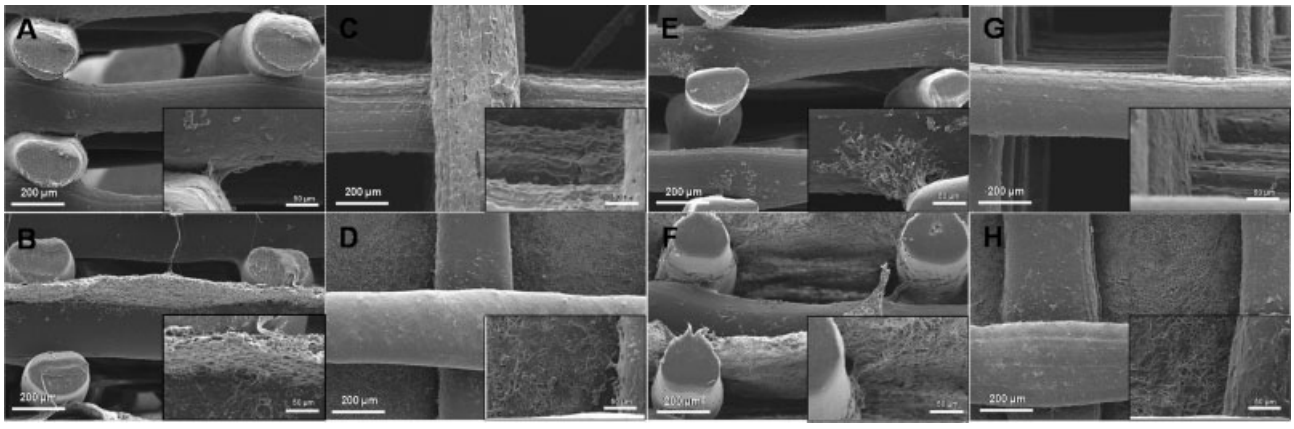

Figure 2. SEM micrographs of rapid prototyped (A, C, E, G) and hierarchical fibrous (B, D, F, H) scaffolds cultured with human osteoblast-like cells (Saos-2 cell line) for 1 (A–D) and 7 (E–H) days. Cross-sections (A, B, E, F) and top views (C, D, G, H) of the constructs. Insets, higher magnifications

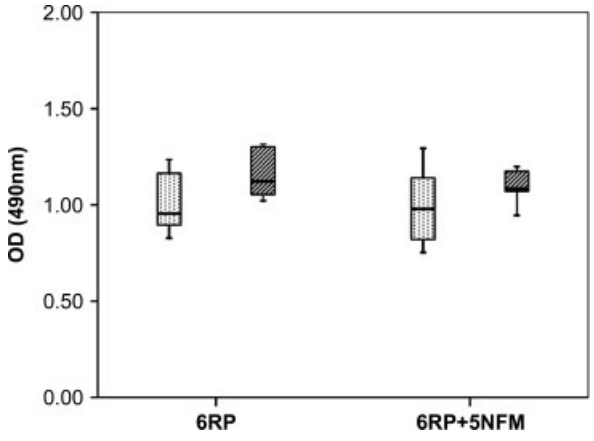

Figure 3. Box plot of cell viability results of human osteoblastic cells cultured on rapid prototyped (6RP) and hierarchical fibrous (6RP + 5NFM) scaffolds for 1 and 7 days. Data were analysed by the non-parametric method of a Kruskal–Wallis test ($p < 0.05$)

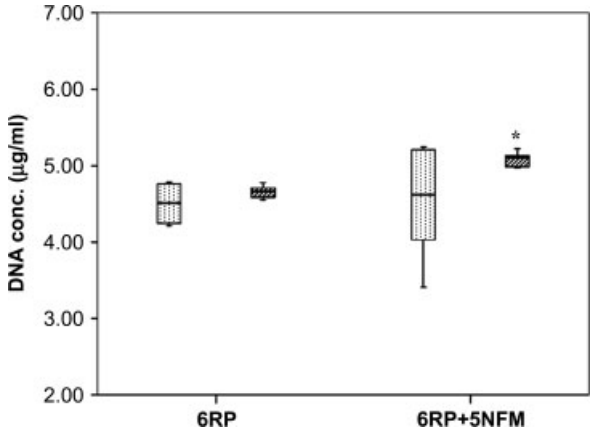

Figure 4. Box plot of DNA content of osteoblast-like cells cultured on rapid prototyped (6RP) and hierarchical fibrous (6RP + 5NFM) scaffolds for 1 and 7 days. Data were analysed by the non-parametric method of a Kruskal–Wallis test; *$p < 0.05$

0.05), especially for longer culture periods. However, for the RP scaffolds, the osteoblastic activity was not maintained throughout the experiment, as observed by a

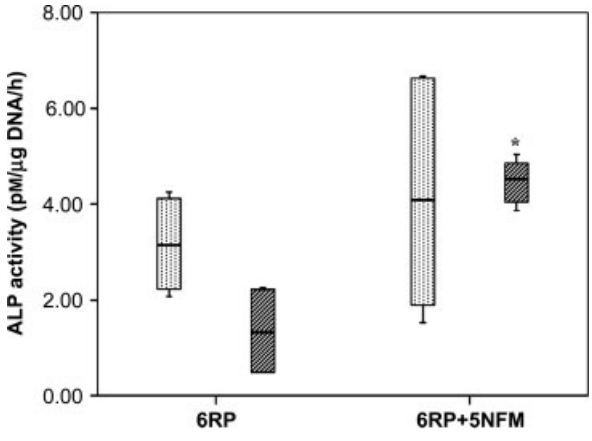

Figure 5. Box plot of ALP activity, normalized against dsDNA amount, from osteoblastic cells (Saos-2 cell line) cultured on rapid prototyped (6RP) and hierarchical fibrous (6RP + 5NFM) scaffolds for 1 and 7 days. Data were analysed by the non-parametric method of a Kruskal–Wallis test; *$p < 0.05$

decrease in ALP activity from day 1 to day 7 of culture. It was previously reported by Schantz *et al*. (2003) that rabbit calvarial osteoblasts, seeded onto PCL scaffolds fabricated via fused deposition modelling (FDM) and embedded into a fibrin matrix (Tisseel, Baxter Hyland Immuno), showed no significant differences in their ALP activity along time. These results are in accordance with those of our study.

4. Conclusion

A novel hierarchical fibrous scaffold was developed, combining starch-polycaprolactone micro- and polycaprolactone nano-motifs, respectively produced by rapid prototyping and electrospinning. It is evident that the nanofiber meshes supply topological cues at the ECM level, whereas the micro 3D fibrous structure provide the required mechanical stability. We here demonstrated that the integration of these two hierarchial structures lead to improved biological performance. Indeed, human

DOI: 10.1002/term

osteoblast-like cells presented significantly higher proliferation and maturation when seeded on these hierarchical starch-based fibrous scaffolds. Overall, the results corroborate our hypothesis that the hierarchical fibrous structure of the scaffolds, mimicking the hierarchical structure of the native ECM, is favourable for bone tissue-engineering strategies.

Acknowledgements

This work was partially supported by the European Integrated Project GENOSTEM (Grant No. LSH-STREP-CT-2003-503161) and the European Network of Excellence EXPERTISSUES (Grant No. NMP3-CT-2004-500283). We also acknowledge the Portuguese Foundation for Science and Technology for the project Naturally Nano (Grant No. POCI/EME/58982/2004) and a PhD grant to A. Martins (Grant No. SFRH/BD/24382/2005).

References

Agrawal CM, Ray RB. 2001; Biodegradable polymeric scaffolds for musculoskeletal tissue engineering. *J Biomed Mater Res* **55**: 141–150.

Araújo JV, Martins A, Leonor IB, *et al*. 2008; Surface controlled biomimetic coating of polycaprolactone nanofibre meshes to be used as bone extracellular matrix analogues. *J Biomater Sci Polym Ed* **19**: 1239–1256.

Capes JS, Ando HY, Cameron RE. 2005; Fabrication of polymeric scaffolds with a controlled distribution of pores. *J Mater Sci Mater Med* **16**: 1069–1075.

Gomes ME, Azevedo HS, Moreira AR, *et al*. 2008; Starch-poly(ε-caprolactone) and starch-poly(lactic acid) fibre-mesh scaffolds for bone tissue engineering applications: structure, mechanical properties and degradation behaviour. *J Tissue Eng Regen Med* **2**: 243–252.

Gomes ME, Holtorf HL, Reis RL, *et al*. 2006; Influence of the porosity of starch-based fibre mesh scaffolds on the proliferation and osteogenic differentiation of bone marrow stromal cells cultured in a flow perfusion bioreactor. *Tissue Eng* **12**: 801–809.

Gomes ME, Reis RL, Cunha AM, *et al*. 2001; Cytocompatibility and response of osteoblastic-like cells to starch-based polymers: effect of several additives and processing conditions. *Biomaterials* **22**: 1911–1917.

Gomes ME, Sikavitsas VI, Behravesh E, *et al*. 2003; Effect of flow perfusion on the osteogenic differentiation of bone marrow stromal cells cultured on starch-based three-dimensional scaffolds. *J Biomed Mater Res A* **67**: 87–95.

Huang ZM, Zhang YZ, Kotaki M, *et al*. 2003; A review on polymer nanofibres by electrospinning and their applications in nanocomposites. *Compos Sci Technol* **63**: 2223–2253.

Hutmacher DW, Schantz JT, Lam CX, *et al*. 2007; State of the art and future directions of scaffold-based bone engineering from a biomaterials perspective. *J Tissue Eng Regen Med* **1**: 245–260.

Hutmacher DW, Sittinger M, Risbud MV. 2004; Scaffold-based tissue engineering: rationale for computer-aided design and solid free-form fabrication systems. *Trends Biotechnol* **22**: 354–362.

Kwon IK, Kidoaki S, Matsuda T. 2005; Electrospun nano- to microfibre fabrics made of biodegradable copolyesters: structural characteristics, mechanical properties and cell adhesion potential. *Biomaterials* **26**: 3929–3939.

Lam CXF, Mo XM, Teoh SH, *et al*. 2002; Scaffold development using 3D printing with a starch-based polymer. *Mater Sci Eng C* **20**: 49–56.

Leong KF, Cheah CM, Chua CK. 2003; Solid freeform fabrication of three-dimensional scaffolds for engineering replacement tissues and organs. *Biomaterials* **24**: 2363–2378.

Lutolf MP, Hubbell JA. 2005; Synthetic biomaterials as instructive extracellular microenvironments for morphogenesis in tissue engineering. *Nature Biotechnol* **23**: 47–55.

Martins A, Araújo JV, Reis RL, *et al*. 2007; Electrospun nanostructured scaffolds for tissue engineering applications. *Nanomedicine* **2**: 929–942.

Mironov V, Boland T, Trusk T, *et al*. 2003; Organ printing: computer-aided jet-based 3D tissue engineering. *Trends Biotechnol* **21**: 157–161.

Moroni L, de Wijn JR, van Blitterswijk CA. 2005; Three-dimensional fibre-deposited PEOT/PBT copolymer scaffolds for tissue engineering: influence of porosity, molecular network mesh size, and swelling in aqueous media on dynamic mechanical properties. *J Biomed Mater Res A* **75**: 957–965.

Moroni L, de Wijn JR, van Blitterswijk CA. 2006; 3D fibre-deposited scaffolds for tissue engineering: influence of pores geometry and architecture on dynamic mechanical properties. *Biomaterials* **27**: 974–985.

Moroni L, Schotel R, Hamann D, *et al*. 2008; 3D fibre-deposited electrospun integrated scaffolds enhance cartilage tissue formation. *Adv Func Mater* **18**: 53–60.

Norman JJ, Desai TA. 2006; Methods for fabrication of nanoscale topography for tissue engineering scaffolds. *Ann Biomed Eng* **34**: 89–101.

Oliveira JT, Crawford A, Mundy JM, *et al*. 2007; A cartilage tissue engineering approach combining starch-polycaprolactone fibre mesh scaffolds with bovine articular chondrocytes. *J Mater Sci Mater Med* **18**: 295–302.

Peltola SM, Melchels FP, Grijpma DW, *et al*. 2008; A review of rapid prototyping techniques for tissue engineering purposes. *Ann Med* **40**: 268–280.

Pfister A, Landers R, Laib A, *et al*. 2004; Biofunctional rapid prototyping for tissue-engineering applications: 3D bioplotting versus 3D printing. *J Polym Sci Part A Polym Chem* **42**: 624–638.

Salgado AJ, Coutinho OP, Reis RL. 2004; Novel starch-based scaffolds for bone tissue engineering: cytotoxicity, cell culture, and protein expression. *Tissue Eng* **10**: 465–474.

Salgado AJ, Coutinho OP, Reis RL, *et al*. 2007; *In vivo* response to starch-based scaffolds designed for bone tissue engineering applications. *J Biomed Mater Res A* **80**: 983–989.

Salgado AJ, Figueiredo JE, Coutinho OP, *et al*. 2005; Biological response to pre-mineralized starch based scaffolds for bone tissue engineering. *J Mater Sci Mater Med* **16**: 267–275.

Santos MI, Fuchs S, Gomes ME, *et al*. 2007; Response of micro- and macrovascular endothelial cells to starch-based fibre meshes for bone tissue engineering. *Biomaterials* **28**: 240–248.

Schantz JT, Teoh SH, Lim TC, *et al*. 2003; Repair of calvarial defects with customized tissue-engineered bone grafts I. Evaluation of osteogenesis in a three-dimensional culture system. *Tissue Eng* **9**: S113–126.

Tuzlakoglu K, Bolgen N, Salgado AJ, *et al*. 2005; Nano- and micro-fibre combined scaffolds: a new architecture for bone tissue engineering. *J Mater Sci Mater Med* **16**: 1099–1104.

Yang F, Murugan R, Wang S, *et al*. 2005; Electrospinning of nano/micro scale poly(L-lactic acid) aligned fibres and their potential in neural tissue engineering. *Biomaterials* **26**: 2603–2610.

Yang S, Leong KF, Du Z, *et al*. 2002; The design of scaffolds for use in tissue engineering. Part II. Rapid prototyping techniques. *Tissue Eng* **8**: 1–11.

Yeong WY, Chua CK, Leong KF, *et al*. 2004; Rapid prototyping in tissue engineering: challenges and potential. *Trends Biotechnol* **22**: 643–652.

Zhang YZ, Lim CT, Ramakrishna S, *et al*. 2005; Recent development of polymer nanofibres for biomedical and biotechnological applications. *J Mater Sci Mater Med* **16**: 933–946.